Towards smaller gap microbulks

2014 JINST 9 C04013

(http://iopscience.iop.org/1748-0221/9/04/C04013)

PUBLISHED BY IOP PUBLISHING FOR SISSA MEDIALAB

RECEIVED: *December 16, 2013*
ACCEPTED: *February 25, 2014*
PUBLISHED: *April 11, 2014*

3rd INTERNATIONAL CONFERENCE ON MICRO PATTERN GASEOUS DETECTORS
1–6 JULY, 2013
ZARAGOZA, SPAIN

2014 JINST 9 C04013

Towards smaller gap microbulks

D. Attié,[a] **L. Boilevin-Kayl,**[a] **T. Dafni,**[b] **E. Ferrer-Ribas,**[a,*] **S. Ferry,**[c] **Y. Giomataris,**[a] **D.C. Herrera,**[b] **F.J. Iguaz,**[a,†] **I.G. Irastorza,**[b] **M. Kebbiri,**[a] **T. Papaevangelou,**[a] **R. de Oliveira,**[c] **L. Seguí**[b,‡] **and A. Tomás**[b,§]

[a] *IRFU, Centre d'Études Nucleaires de Saclay, (CEA-Saclay), Gif-sur-Yvette, France*
[b] *Instituto de Física Nuclear y Altas Energías, Universidad de Zaragoza, Zaragoza, Spain*
[c] *European Organization for Nuclear Research (CERN), Genève, Switzerland*

E-mail: esther.ferrer-ribas@cea.fr

ABSTRACT: Small gap Micromegas detectors ($< 50\,\mu$m) are expected to be optimal for high pressure applications. Combining the microbulk manufacturing technique with a small gap can result in attractive detectors for rare event detection, in particular double beta decay or dark matter searches. We present novel results obtained with small gap microbulks (25 and 12.5 μm) that have been manufactured recently. For the first time for this type of detectors, we show experimentally that for each amplification gap there is an optimal pressure and that smaller gaps are more suitable for higher pressures.

KEYWORDS: Gaseous detectors; Micropattern gaseous detectors (MSGC, GEM, THGEM, RETHGEM, MHSP, MICROPIC, MICROMEGAS, InGrid, etc); Particle tracking detectors (Gaseous detectors); Dark Matter detectors (WIMPs, axions, etc.)

*Corresponding author.
†Present address: Instituto de Física Nuclear y Altas Energías, Universidad de Zaragoza, Zaragoza, Spain.
‡Present address: University of Oxford, Oxford, United Kingdom.
§Present address: Brackett Laboratory, Imperial College, United Kingdom.

doi:10.1088/1748-0221/9/04/C04013

Contents

1 Introduction

Exploring new physics in particle or nuclear physics needs high performance detectors. The microbulk [1] is a new gaseous detector based on the Micromegas structure [2], which is now a mature technology used in different experiments such as CAST, NEXT, NTOF. The Micromegas gap is fabricated by etching of a polyimide layer, usually 50 μm thick, sandwitched between two thin metallic layers. The high accuracy of this process provides a high precision avalanche gap and it reduces gain fluctuations with improved energy resolution and detector stability. The outcome is a low-mass detector, a key element in many applications while at the same time the use of clean raw-materials provides a unique feature of an intrinsically radiopure detector [4, 5].

In solar axion search (CAST experiment at CERN [6]) the microbulk is used as a low background X-ray detector since 2008. It has shown remarkable operation stability and an extremely low background level at low energy. In neutrinoless double beta decay experiments using a high pressure Xenon TPC the microbulk could be a precious tool due to its low background and enhanced energy resolution capability; developments are in progress in the context of the NEXT experiment [7–9]. In nuclear physics investigations (NTOF experiment) the low material is of paramount importance in order to provide a "neutron transparent" detector for measuring on-line neutron flux and neutron beam profile [10–12].

In previous investigations [3], it was shown that small gap Micromegas detectors would be optimum for operation at high pressure where the gain could be maximised and fluctuations due to geometrical factors or environmental ones would be cancelled. This property is important in the field of rare event searches in order to increase the sensitivity and, in the case of Xenon gas, to enhance detection efficiency of gamma rays. In [13] characterization of microbulk detectors was investigated with different gas mixtures in Argon and neon for 50 and 25 μm gaps. In the present work the study is extended down to 12.5 μm.

2014 JINST 9 C04013

Table 1. Summary of the pattern of holes diameters and pitchs for the three different amplification gaps of the tested detectors.

amplification gap (μm)	hole diameter (μm)	hole pitch (μm)
12.5	25	80
25	30	100
50	40	90

The paper is organised as follows: section 2 describes briefly the microbulk fabrication process and the mesh geometry of the studied detectors. In addition electric field simulations are presented to understand experimental results obtained with various avalanche gaps indicating the technological roadmap for future optimization of the microbulk detector. Section 3 is devoted to the performance of 25 and 12.5 μm gap microbulks compared to 50 μm including gain and energy resolution. Novel results are shown exhibiting the relation of amplification gap versus gas pressure. Finally conclusions and perspectives are discussed in section 4.

2 Fabrication process and mesh geometry considerations

The manufacturing process of a microbulk detector was described in detail in [1]. Here we only remind the main three steps in figure 1. The raw material is a thin flexible kapton foil (of 25 μm or 12.5 μm) with a 5 μm copper layer on each side (figure 1 step 1). A thin photoresistive film is laminated on top of the kapton foil and it is illuminated by UV light to produce the required mask (figure 1 step 2). The copper is then removed by a standard lithographic process and the non-illuminated regions produce a pattern of a thin mesh. The polyimide is then etched and partially removed in order to create tiny pillars in the shadow part of the mesh below the copper mesh. In the prototypes used here the holes are 30 (25) μm in diameter with a pitch of 100 (80)μm for the 25 (12.5) μm amplification gaps in a hexagonal pattern to optimise electron transmission. A summary of the geometry of the holes diameters and pitch for the different amplifications gaps is given in table 1.

In 50 μm gap Micromegas detectors, the holes diameter is usually conceived smaller than the amplification gap to favor the funnel electric field effect. In the case of the present detectors with gaps of 25 and 12 .5 μm this is not possible. The limitation comes from the attainable precision on the mask films that define the minimum mesh holes diameter. This limitation could be exceeded by an alternative more expensive technique, using glass masks, where holes of 20 μm diameter could be achieved. Going further with the present techniques seems difficult.

In order to verify that the thickness of the mesh as well as the diameter of the holes will not perturb the shape of the electric field lines, a field simulation was effectuated using the Lorentz software package [14]. In figure 2 the field line configuration is shown for the 12.5 and 25 μm amplification gap with a simplified geometry. The insulating kapton pillars have not been considered for these simulations. The typical funnel shape of the field lines at the mesh hole entrances seems well preserved. However figure 3 shows the magnitude of the electric field at different heights within the amplification gaps across the hole as indicated in the sketch of figure 3. The depicted

2014 JINST 9 C04013

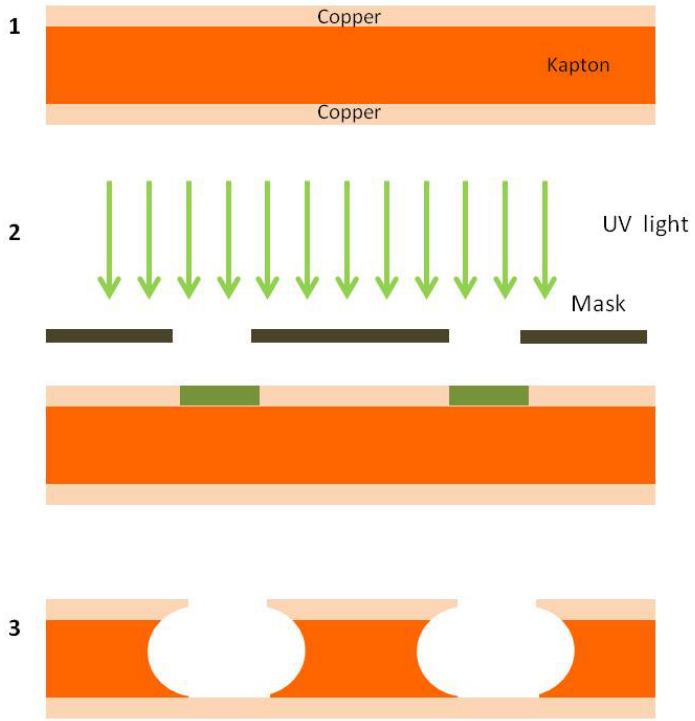

Figure 1. Summary of the manufacturing process of a single anode microbulk, described in the text.

electric field ranges from 99% (black points) to 1% (pink points) of the amplification gap for the three different cases (12.5, 25 and 50 μm). The 99% correspond to heights at the level of the mesh while heights of 1% correspond to heights close to the anode, where the electric field is the strongest. The voltage applied is the same for the different gaps and only relative differences are pertinent here.

If we compare the ratio of the field at 99% and 1% of the amplification gap for the different gaps, we observe that for the 50 μm gap this ratio is 1.77 while for the 12.5 μm is 1.49. This means that the increase of the field near the anode for the small gaps is smaller than for the larger gaps with this hole geometry. This will probably lead to reduced gains for the small gaps. This effect would be corrected if the diameter of the holes could be reduced.

The second consideration is that for the small gaps there is greater dispersion of the magnitude of the electric field close to the anode i.e for the 50 μm the magnitude of the electric field is nearly constant from heights greater than 50%. Another way of seeing this effect, is by looking at the integration of the electric field across the amplification gap. Figure 4 shows the integrated electric field across the amplification gap at two different positions: at the middle of the hole and a position shifted of 15% to one side as shown in the sketch. The difference between the two curves is greater for the small gaps than for the 50 μm. In particular the difference between the integration of the two positions at the level of the anode at the maximum of the electric field is only of 1% while for the 12.5 μm amplification gap the difference reaches 8%. In addition, the averaged integrated field ratio between the two positions is of 12% for the 12.5 μm amplification gap and only of 5% for the 50 μm amplification gap meaning that the avalanche will take place in a similar manner regardless

2014 JINST 9 C04013

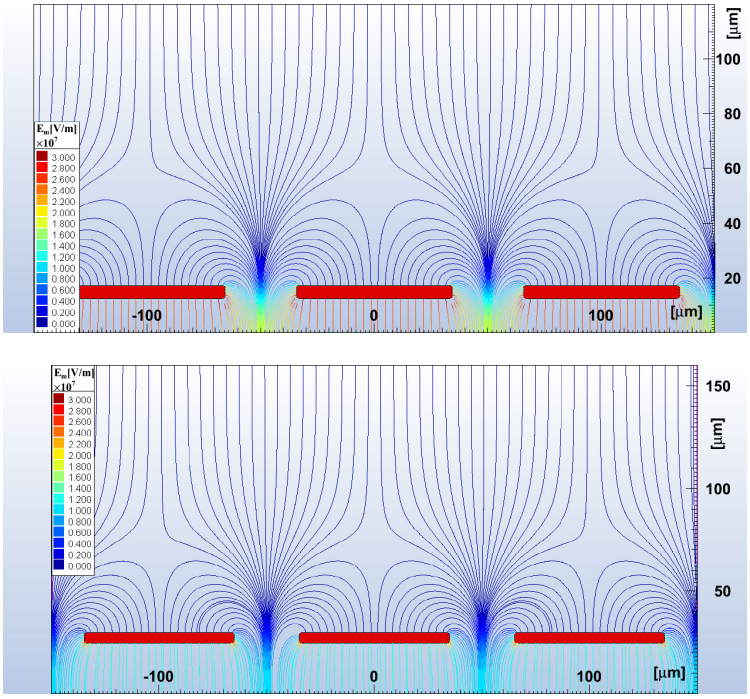

Figure 2. Field line simulation of a 12.5 and 25 μm amplification gap Micromegas detector with the hole and pitch dimensions described in table 1.

of position within the hole for the 50 μm amplification gap. This fact will probably have an effect on the energy resolution.

3 Performances of 12.5 and 25 μm gap microbulks compared to 50 μm

The microbulks of 50 μm are relatively well-known. They have been well characterised [1, 7, 13] and are being used in the CAST experiment [1], in the R&D for the NEXT experiment [8] and in the NTOF [10]. In the next section we will compare the performance of the novel small gap microbulk with respect to the well known 50 μm amplification gap ones. In particular, it is the first time that the behaviour of smaller gap microbulks as a function of pressure (from 0.4 bar to 1.7 bar) is studied in Argon-Isobutane mixtures.

3.1 Set-up description

The detectors were installed in an aluminium vessel with an aluminized mylar window allowing calibration by X-rays from an ^{55}Fe source. The prototypes used in these tests are single anode round detectors with an active zone of a diameter of 35 mm. A picture of the detector and a zoom of the active area are shown in figure 5. The gas mixture was allowed to circulate for several hours before each measurement and at every change of the gas mixture or the pressure. To maintain the drift gap, a mesh frame is layed on 10 mm pillars. The mesh signal was read out by an ORTEC 142B preamplifier followed by a CANBERRA 2022 Spectroscopy amplifier. The pulse height distributions are recorded by a multi-channel analyzer AMPTEK MCA-8000A. Each spectrum

2014 JINST 9 C04013

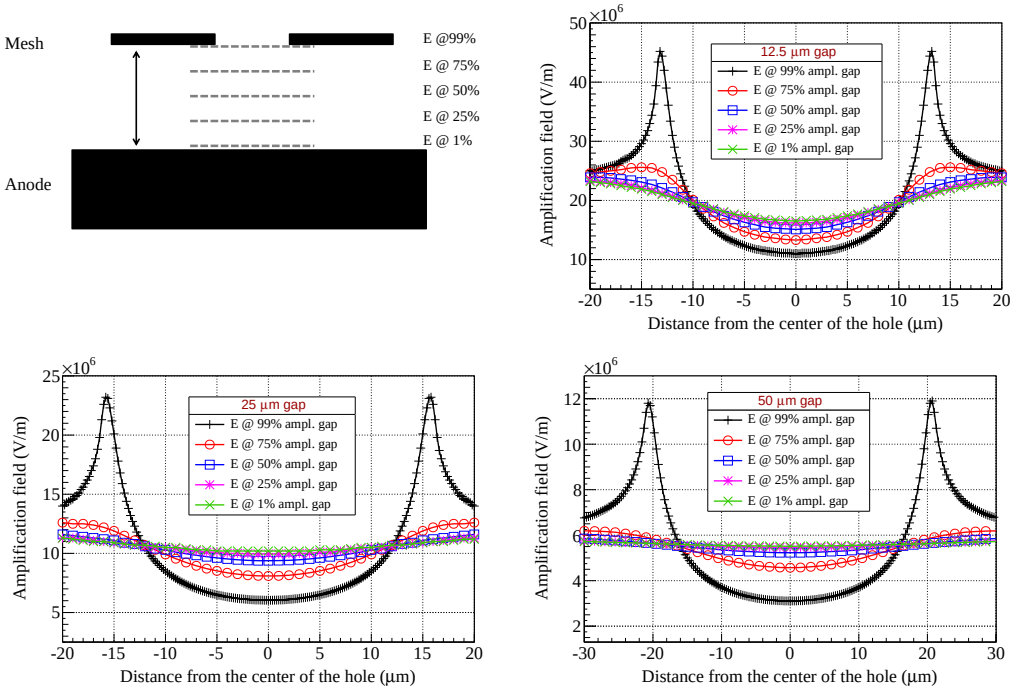

Figure 3. Sketch to illustrate the electrostatic simulation (top left). Magnitude of the electric field at different heights within the amplification holes for the 12 (top right), 25 (bottom left) and 50 (bottom right) μm amplification gaps.

was fitted by two Gaussian functions, corresponding to the K_α (5.9 keV) and K_β (6.4 keV) lines of the ^{55}Fe source; the mean position and width of the main peak were obtained for each fit.

3.2 Measurements at atmospheric pressure

3.2.1 Gain

The 25 and 12.5 μm detectors were tested at atmospheric pressure with different percentages of Isobutane. A scan of the drift field was done at fixed amplification field in order to obtain the electron transmission and to find the range of optimal operation. The result is shown in figure 6 exhibiting a similar behaviour for the two different gaps. It is noteworthy that there is a wide range of ratios of drift and amplification fields, where the relative electron transmission is greater than 90%. The region where the electron transmission is constant, called the plateau, is extended when the percentage of Isobutane is increased [15]. This effect is correlated with the diffusion coefficient and was already verified in [7, 13, 20]. On the other hand, there is a steady increase of the gain with the drift field that is more prominent at high Isobutane concentrations and for the 12.5 μm gap. This effect was already observed in [13] and has been simulated with the neBEM and Garfield [16, 17]. At high drift fields, the mesh stops being transparent as some of the field lines stop at the mesh and part of the electrons are lost.

In order to obtain the gain of the detector as a function of amplification field, the ratio of drift and amplification field is set at the maximum of transmission. Figure 7 shows the gain versus

2014 JINST 9 C04013

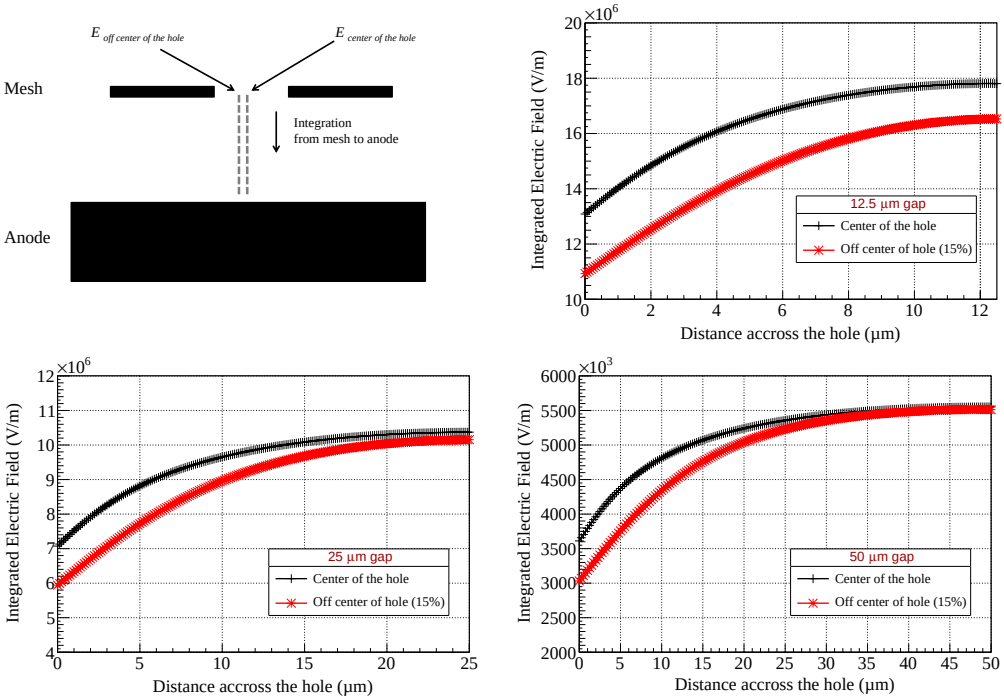

Figure 4. Integrated electric field across the amplification gap for the 12 (a), 25 (b) and 50 (c) μm amplification gaps. The full line corresponds to the integrated electric field at the center of the hole whilst the dashed line corresponds to the integrated field shifted of 15% from the center of the hole.

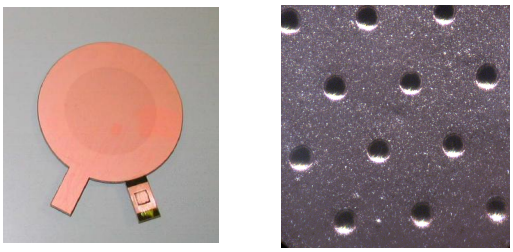

Figure 5. Left: picture of a 3.5 cm diameter circular microbulk used in these tests. Right: zoom of the active area. The hexagonal pattern of the 30 μm diameter mesh holes with a pitch of 100 μm can be observed.

amplification fields for different gas mixtures for 12.5 μm (left) and 25 μm (right) amplification gaps. Gains greater than 7×10^3 are obtained for the 12.5 μm gap. For the 25 μm, the maximum gains reach 10^4 for concentrations of 15% and 20%. The maximum gains observed are below the sparking point of the detector, i.e the detectors have not been pushed to the limit. The results for the 25 μm detectors corroborate the previous measurements in [13]. In order to have a common point of comparison, figure 8 shows the gain for the three different gaps in the same conditions, at atmospheric pressure in an Ar + 10% Isobutane mixture showing that the highest gains are obtained for the 50 μm gap despite the lowest electric field applied as the distance for the avalanche to develop is larger.

2014 JINST 9 C04013

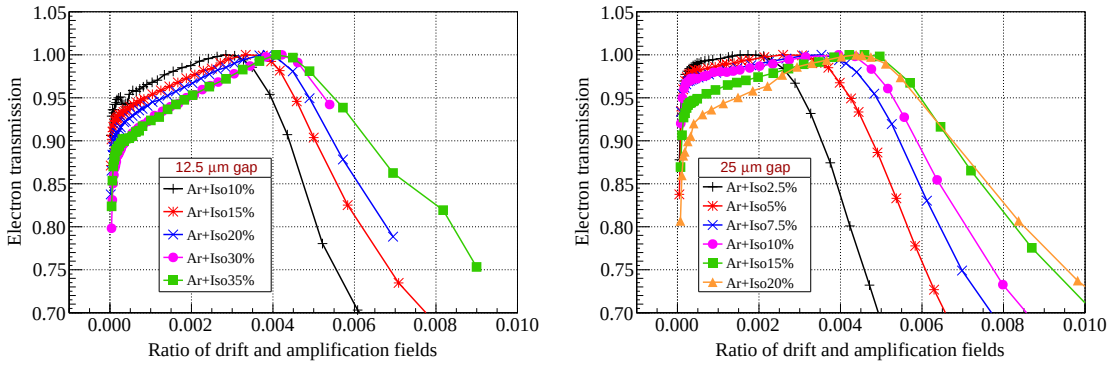

Figure 6. Electron transmission versus ratio of drift and amplification fields for different gas mixtures for 12.5 μm (left) and 25 μm (right) amplification gaps.

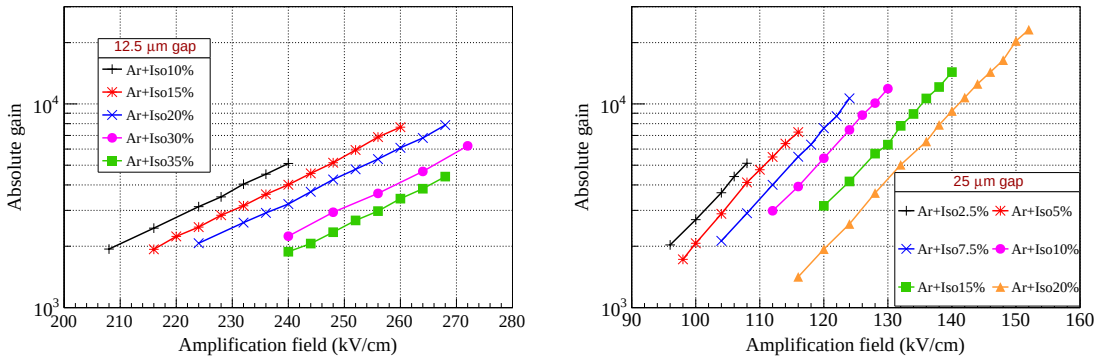

Figure 7. Gain versus amplification fields for different gas mixtures for 12.5 μm and 25 μm amplification gaps.

3.2.2 Energy resolution measurements

The energy resolution has been studied for different concentrations of Isobutane. The results are shown in figure 9. For a given gas mixture the energy resolution increases with gain as the signal to noise ratio is increased. Normally a minimum is reached and at high gain a degradation can be observed due to the extra fluctuations [18]. This degradation is not observed neither for the 12.5 μm nor for the 25 μm. As in the gains studies, detectors have not been pushed to the sparking limit.

Regarding the percentage of quencher, at low concentrations the energy resolution is worse as not all the UV photons in the avalanche are absorbed. The best energy resolution is obtained at Ar + 10% Isobutane and Ar + 20% mixtures for the 25 μm and12.5 μm respectively. These concentrations, that seem optimum for the energy resolution, will be the reference ones to study the performance as a function of pressure in the next section.

In order to obtained the ultimate energy resolution we have repeated the measurement using a chrome foil in order to select the K_α (5.9 keV) line of the ^{55}Fe. This is shown in figure 10. We can see that these values, 12% and 11% for the 25 and 50 μm gaps respectively are close to the theoretical limitations and do not depend on our fitting procedure.

2014 JINST 9 C04013

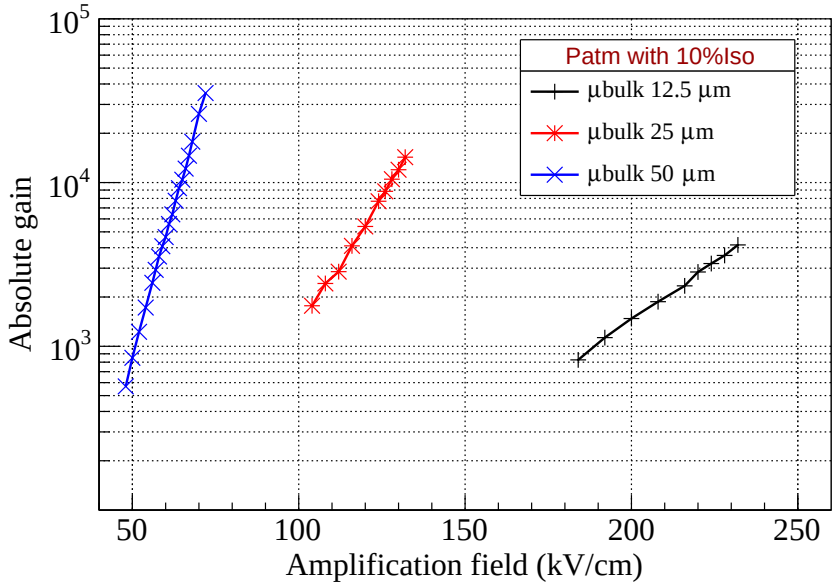

Figure 8. Comparison of gain for the different gaps at atmospheric pressure in Ar + 10% Isobutane.

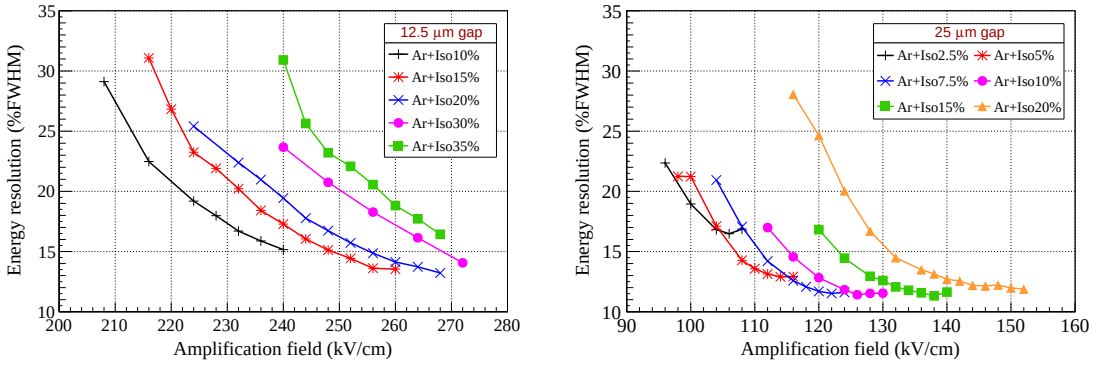

Figure 9. Resolution versus amplification fields for different gas mixtures for 12.5 μm and 25 μm amplification gaps.

This is observed by calculating the lower limit on the obtainable energy resolution in gas detectors taking into account primary and avalanche fluctuations. It can be written as follows:

$$\frac{\sigma_E}{E}(FWHM) = 2.35\sqrt{\frac{W}{E_0}(F+b)}, \tag{3.1}$$

where W is the mean energy per ion pair, E_0 is the initial total energy of the ionization particle, F is the Fano factor and b is the relative variance for the distribution of the number of electrons produced in a single avalanche. Using typical values of $F = 0.2$, $W = 25\,\text{eV}$ and $b = 0.5$ [19], the minimum resolution at 5.9 keV is 10.8% (FWHM).

2014 JINST 9 C04013

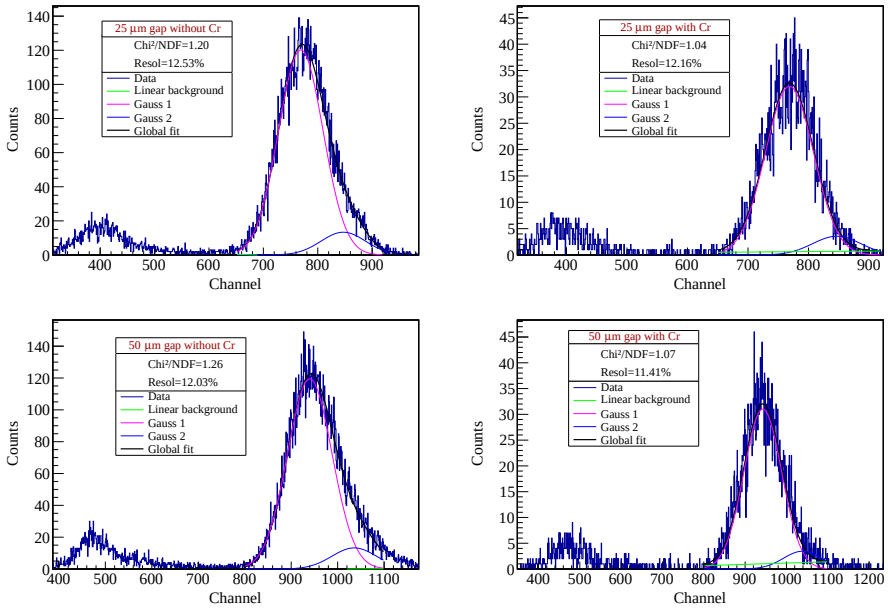

Figure 10. Comparison of the energy resolution for the 25 and 50 μm amplification gaps without (left) and with (right) a chrome foil. The chrome foil selects the K_α (5.9 keV) line.

3.3 Performance versus pressure

The motivation for this study is to show experimentally that there is an optimal range of pressures for operation for every amplification gap. This theory was shown in [3] by the Townsend coefficient in the Rose-Korff's parametrisation [22]:

$$\alpha = PAe^{\frac{-BP}{E}} \tag{3.2}$$

where P is the gas pressure, A and B are parameters that depend on the gas and E is the electric field. The gain can be then written as:

$$G = \exp\left(PAe^{\frac{-BPd}{E}}\right) = \exp\left(PAe^{\frac{-BPd}{V}}\right) \tag{3.3}$$

with V being the applied voltage. We recall here that this expression can be differentiated in order to find a set of parameters (pressure and voltage) that will optimise the stability operation:

$$\frac{\partial G}{\partial P} = G\alpha\left(1 - \frac{BPd}{V}\right) \tag{3.4}$$

We can then deduce, by setting 3.4 equal to 0, that for each gap there is an optimal pressure that can be written as:

$$P = \frac{V}{Bd} \tag{3.5}$$

From this relation, we can see that the pressure is inversely proportional to the amplification gap, so it is expected that small amplification gaps will be more suitable for operation at higher pressures. In [20] this idea was done by testing different Micromegas detectors of the Ingrid [21] type with gaps from 45 μm to 68 μm at fixed gas conditions to observe the evolution of the gain at a given voltage. Here the gain for the three different gaps has been measured at different pressure conditions. The gas mixture that optimises the behaviour for each gap in terms of energy resolution

2014 JINST 9 C04013

and gain have been chosen. The curves are shown in figure 11 for various pressures and Isobutane percentages: 20%, 10% and 5% for 12.5, 25 and 50 μm amplification gaps.

The pressure has been scanned from 0.5 to 1.7 bar. The gains achieved in this range are greater than 5×10^4 for the 12.5 μm gap and 10^4 for the 25 μm gap. For the 50 μm gap the gains are as high as 3×10^4 and no degradation is seen with the pressure. The trend for the energy resolution as a function of electric field is shown in figure 12. The best minimum is between 11 and 13% for the three gaps. A summary of these results can be seen figure 12 where the evolution of the gain and the energy resolution as a function of pressure is given for a fixed electric field. The gain follows the expected bell shape with a shifting maximum with amplification gap. The best value of energy resolution is reached at the maximum of the gain [3]. The optimum range of pressures is 0.4 bar for the 50 μm gap, 0.7 bar for the 25 μm gap while for the 12.5 bar is 0.9 bar confirming that smaller gaps are optimum for higer pressures. As these measurements have been performed in different Argon-Isobutane mixtures (5% Isobutane, 10% Isobutane and 20% for the 50 μm, 25 μm and 12.5 μm respectively) in order to optimise the energy resolution, we have verified that at fixed gas mixture (with B of equation (3.4) fixed) the trend is the same. Figure 13 shows the evolution of the gain and the energy resolution as a function of pressure for a gas mixture of Argon+10%Isobutane. The general trend is the same as in figure 12. However the maximum for the 12.5 μm amplification gap is slightly shifted to a higher pressure and the resolution is $\sim$ 14% instead of $\sim$ 12%. Concerning the 50 μm amplification gap the maximum has not been reached, as lower pressures were needed that were not reachable but the resolution reamins unchanged ($\sim$ 11%).

In figure 14 the best energy resolution at each pressure is shown independently of the electric field applied. The range of pressure where the behaviour is optimal is within $\pm$0.1 bar around the minimum and is broader for the 12.5 and 25 μm gaps. In addition, this figure indicates that the optimum gap in an Argon-Isobutane mixture at atmospheric pressure is probably 25 μm.

4 Conclusion and perspectives

Microbulk detectors of 25 and 12.5 μm amplification gap have been manufactured and tested with success. Gains greater than 10^4 for the 25 μm detectors and 8×10^3 for the 12.5 μm have been obtained in Argon-Isobutane mixtures. Energy resolutions as low as 12% (FWHM) for the 12.5 μm while for the 25 μm values of 11.5% have been reached at 5.9 keV. These values are very close to the minimum energy resolution that can be achieved with gaseous detectors taking into account the fluctuations due to electron multiplication. The electric field simulations qualitatively indicate that the differences in the gain and resolution of the two detector types could be due to the holes pattern and the manufacturing limitations of the smallest gaps.

The behaviour of these detectors has also been studied as a function of pressure from 0.5 bar to 1.7 bar. The gain follows the expected bell shape with the maximum shifted with the pressure: smaller gaps are more suitable for higher pressures.

These tests confirm the suitability of small gap microbulk for rare event detection that would require operation pressures above the atmospheric.

Acknowledgments

We would like to thank Denis Bernard for fruitful comments on the manuscript.

2014 JINST 9 C04013

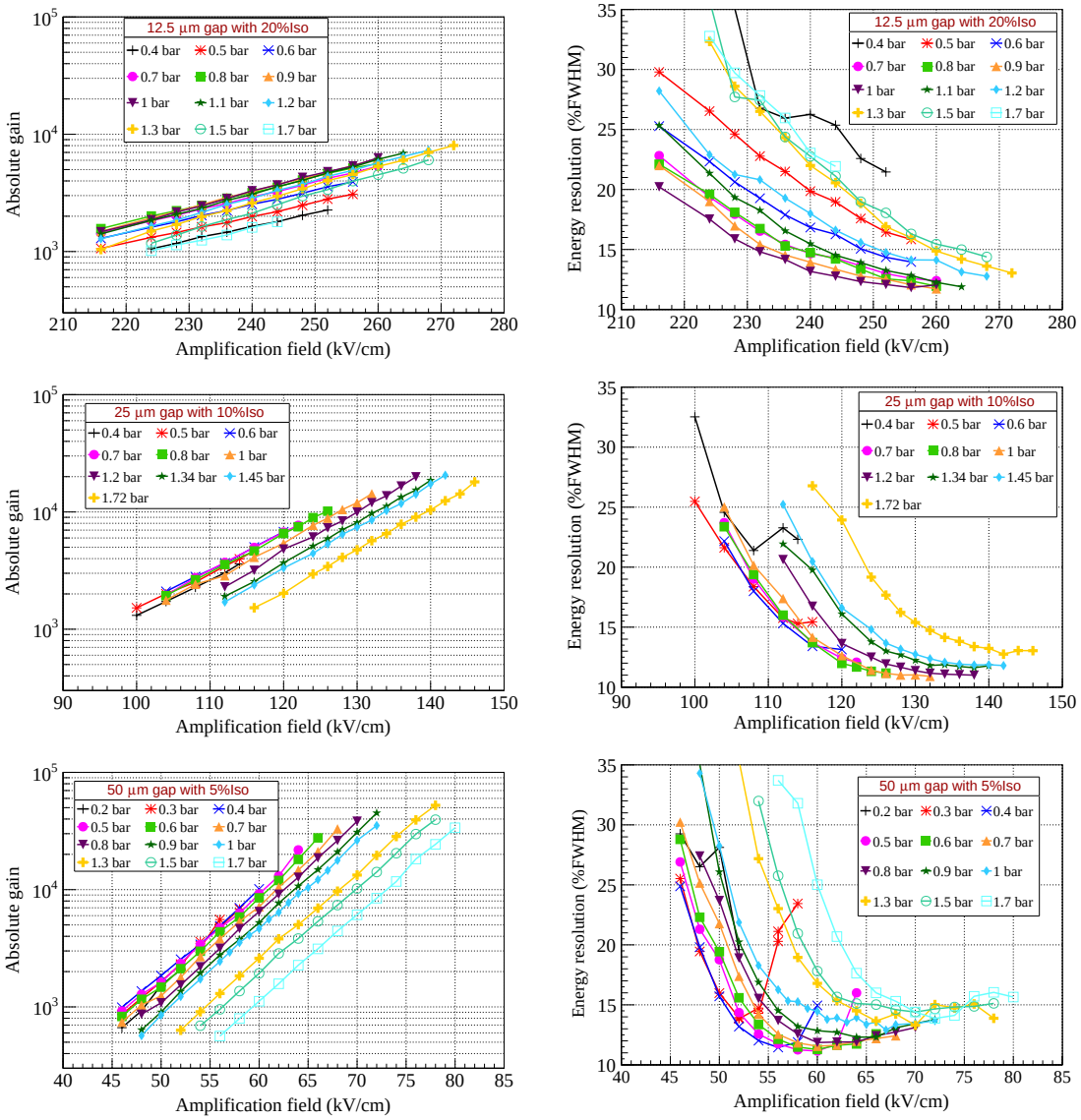

Figure 11. Gain measurements (left) and energy resolution (right) for different pressures in Argon-Isobutane mixtures: 20% for 12.5 μm , 10% for 25 μm and 5% for 50 μm amplification gaps.

2014 JINST 9 C04013

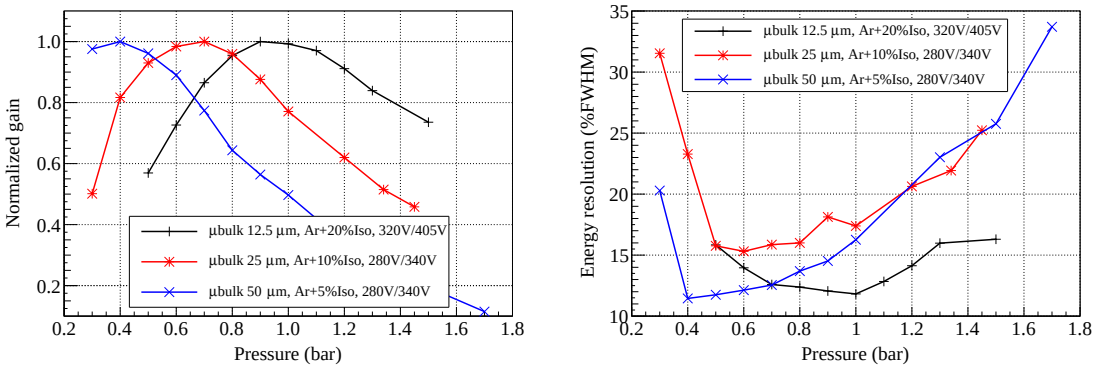

Figure 12. Gain (left) and resolution (right) versus pressure at a given amplification field for each detector gap in Argon-Isobutane mixtures: 20% for 12.5 μm , 10% for 25 μm and 5% for 50 μm amplification gaps.

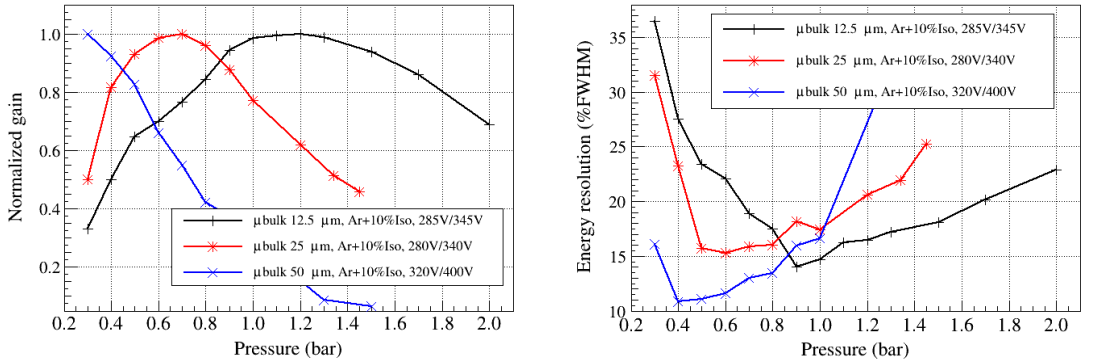

Figure 13. Gain (left) and resolution (right) versus pressure for 50 μm, 25 μm and 12.5 μm at a given amplification field for each detector gap for an Argon-10% Isobutane mixture.

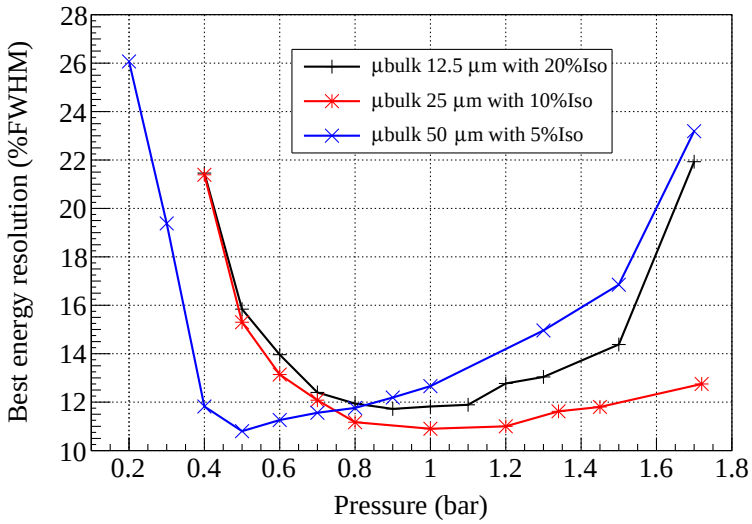

Figure 14. Best energy resolution versus pressure for 50 μm, 25 μm and 12.5 μm amplification gaps at a given amplification field for each detector gap.

2014 JINST 9 C04013

References

[1] S. Andriamonje et al., *Development and performance of Microbulk Micromegas detectors*, 2010 *JINST* **5** P02001

[2] Y. Giomataris, P. Rebourgeard, J.P. Robert and G. Charpak, *MicrOMEGAs: A High granularity position sensitive gaseous detector for high particle flux environments*, *Nucl. Instrum. Meth.* **A 376** (1996) 29 [INSPIRE].

[3] Y. Giomataris, *Development and prospects of the new gaseous detector 'MicrOMEGAs'*, *Nucl. Instrum. Meth.* **A 419** (1998) 239 [INSPIRE].

[4] I.G. Irastorza, E. Ferrer Ribas and T. Dafni, *Micromegas in the rare event searches*, *Mod. Phys. Lett.* **A 28** (2013) 1340026.

[5] S. Cebrián, T. Dafni, E. Ferrer-Ribas, J. Galan, I. Giomataris et al., *Radiopurity of MicrOMEGAs readout planes*, *Astropart. Phys.* **34** (2011) 354 [arXiv:1005.2022].

[6] S. Aune, J.F. Castel, T. Dafni, M. Davenport, G. Fanourakis et al., *Low background x-ray detection with MicrOMEGAs for axion research*, 2014 *JINST* **9** P01001 [arXiv:1310.3391].

[7] T. Dafni, E. Ferrer-Ribas, I. Giomataris, P. Gorodetzky, F. Iguaz et al., *Energy resolution of alpha particles in a microbulk MicrOMEGAs detector at high pressure Argon and Xenon mixtures*, *Nucl. Instrum. Meth.* **A 608** (2009) 259 [arXiv:0906.0534].

[8] S. Cebrián et al., *Micromegas-TPC operation at high pressure in xenon-trimethylamine mixtures*, 2013 *JINST* **8** P01012.

[9] THE NEXT collaboration, V. Alvarez et al., *Characterization of a medium size Xe/TMA TPC instrumented with microbulk MicrOMEGAs, using low-energy γ-rays*, arXiv:1311.3535 [INSPIRE].

[10] F. Belloni et al., *Micromegas for neutron detection and imaging* , *Mod. Phys. Lett.* **A 28** (2013) 1340023.

[11] S. Andriamonje et al., *A Transparent Detector for n TOF Neutron Beam Monitoring J. Korean Phys. Soc.* **59** (2011) 1597.

[12] C. Guerrero et al., *Simultaneous measurement of neutron-induced capture and fission reactions at CERN*, *Eur. Phys. J.* **A** (2012) 48: 29.

[13] F.J. Iguaz, E. Ferrer Ribas and Y. Giomataris, *Characterization of microbulk detectors in Argon- and neon-based mixtures*, 2012 *JINST* **7** P04007.

[14] Integrated Engineering Software, http://www.integratedsoft.com/.

[15] A. Tomás Alquezar, *Development of Time Projection Chambers with Micromegas for Rare Event Searches.*, Ph.D. Thesis, 2013 JINST TH 001, Laboratorio de Física Nuclear y Astropartículas, Departemento de Física Teórica, Universidad de Zaragoza (2013).

[16] P. Bhattacharya et al., *Performance Studies of BULK Micromegas with Different Amplification Gaps*, in proceeding of *3rd International Conference on Micro Pattern Gaseous Detectors*, 1–6 July, 2013, Zaragoza, Spain.

[17] P. Bhattacharya et al.,*Characteristic Studies of Micromegas*, presentation at the RD51 meeting 14-17 October 2013.

[18] I.K Bronic and B. Grosswendt, *Gas amplification and ionization coefficients in Isobutane and Argon-Isobutane mixtures at low gas pressures*, *Nucl. Instrum. Meth.* **B 142** (1998) 219.

[19] W. Blum and L. Rolandi, *Particle detection with drift chambers*, Springer-Verlag (1993).

2014 JINST 9 C04013

[20] M. Chefdeville, *Development of Micromegas-like gaseous detectors using a pixel readout chip as collecting anode*, Ph.D. Thesis, University of Amsterdam (2009).

[21] M. Chefdeville, H. van der Graaf, S. van der Putten, J. Timmermans, J.L. Visschers et al., *An electron-multiplying 'MicrOMEGAs' grid made in silicon wafer post-processing technology*, *Nucl. Instrum. Meth.* **A 556** (2006) 490.

[22] M.E. Rose and S.A. Korff, *An Investigation of the Properties of Proportional Counters*, *P*hys. Rev. **59** (1941) 850.

2014 JINST 9 C04013